# Lawrence Berkeley National Laboratory

**Title**
Unraveling the Main Chain and Side Chain Effects on Thin Film Morphology and Charge Transport in Quinoidal Conjugated Polymers

**Permalink**
https://escholarship.org/uc/item/1rv208g1

**Journal**
Advanced Functional Materials, 28(31)

**ISSN**
1616-301X

**Authors**
Liu, Xuncheng
He, Bo
Garzón-Ruiz, Andrés
et al.

**Publication Date**
2018-08-01

**DOI**
10.1002/adfm.201801874

Peer reviewed

---------------------------------------------------------------------------------------------------------------------------------------------

Dear Author,

**Please correct your galley proofs carefully and return them no more than four days after the page proofs have been received.**

**Please limit corrections to errors already in the text; cost incurred for any further changes or additions will be charged to the author, unless such changes have been agreed upon by the editor.**

The editors reserve the right to publish your article without your corrections if the proofs do not arrive in time.

Note that the author is liable for damages arising from incorrect statements, including misprints.

Please note any queries that require your attention. These are indicated with a Q in the PDF and a question at the end of the document.

**Reprints** may be ordered by filling out the accompanying form.

Return the reprint order form by fax or by e-mail with the corrected proofs, to Wiley-VCH : **afm@wiley.com**

To avoid commonly occurring errors, **please ensure that the following important items are correct** in your proofs (please note that once your article is published online, no further corrections can be made):

- **Names** of all authors present and spelled correctly

- **Titles** of authors correct (Prof. or Dr. only: please note, Prof. Dr. is not used in the journals)

- **Addresses** and **postcodes** correct

- **E-mail address** of corresponding author correct (current email address)

- **Funding bodies** included and grant numbers accurate

- **Title** of article OK

- All **figures** included

- **Equations** correct (symbols and sub/superscripts)

**Corrections should be made directly in the PDF file using the PDF annotation tools. If you have questions about this, please contact the editorial office. The corrected PDF and any accompanying files should be uploaded to the journal's Editorial Manager site.**

# Author Query Form

WILEY

| | | |
|---|---|---|
| Journal | ADFM | |
| Article | adfm201801874 | |

Dear Author,

During the copyediting of your manuscript the following queries arose.

Please refer to the query reference callout numbers in the page proofs and respond to each by marking the necessary comments using the PDF annotation tools.

Please remember illegible or unclear comments and corrections may delay publication.

Many thanks for your assistance.

| Query No. | Description | Remarks |
|---|---|---|
| Q1 | Please provide TOC keyword. | |
| Q2 | Please confirm that forenames/given names (blue) and surnames/family names (vermilion) have been identified correctly. | |
| Q3 | Please provide the highest academic title (either Dr. or Prof.) for all authors, where applicable. | |
| Q4 | Figure 2 citation is missing in the text please check. | |

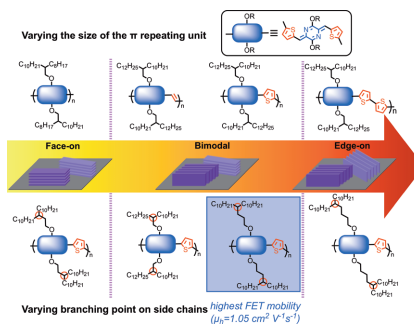**Author: Please confirm that Funding Information has been identified correctly.**

Please confirm that the funding sponsor list below was correctly extracted from your article: that it includes all funders and that the text has been matched to the correct FundRef Registry organization names. If a name was not found in the FundRef registry, it may not be the canonical name form, it may be a program name rather than an organization name, or it may be an organization not yet included in FundRef Registry. If you know of another name form or a parent organization name for a "not found" item on this list below, please share that information.

| FundRef Name | FundRef Organization Name |
|---|---|
| Office of Science | Office of Science |
| Office of Basic Energy Sciences | |
| U.S. Department of Energy | U.S. Department of Energy |
| U.S. Department of Energy | U.S. Department of Energy |
| Office of Science | Office of Science |
| Office of Basic Energy Sciences | |
| Materials Sciences and Engineering Division | |
| Inorganic/Organic Nanocomposites Program | |
| Advanced Light Source | |
| ALS | ALS Society of Canada |
| Office of Science | Office of Science |
| Office of Basic Energy Sciences | |
| U.S. Department of Energy | U.S. Department of Energy |
| China Scholarship Council | China Scholarship Council |
| National Natural Science Foundation of China | National Natural Science Foundation of China |
| CSIRC | |

X. Liu, B. He, A. Garzón-Ruiz,
A. Navarro, T. L. Chen,
M. A. Kolaczkowski, S. Feng,
L. Zhang, C. A. Anderson,
J. Chen,* Y. Liu* ....................... 1801874

**Unraveling the Main Chain and Side Chain Effects on Thin Film Morphology and Charge Transport in Quinoidal Conjugated Polymers**



Varying the size of the π repeating unit

Face-on    Bimodal    Edge-on

Varying branching point on side chains — highest FET mobility ($\mu_h$=1.05 cm$^2$ V$^{-1}$s$^{-1}$)

**Comparative studies of series of quinoidal polymers** with varying main chain or side chain moieties have provided a comprehensive description of the relationship between polymer structures, thin film morphologies, and charge transport properties. A compound "odd-even" branching point effect is observed experimentally and elucidated theoretically. Such studies provide a unique insight for the future design of high-performing organic semiconductors.

# Unraveling the Main Chain and Side Chain Effects on Thin Film Morphology and Charge Transport in Quinoidal Conjugated Polymers

Q2

*Xuncheng Liu, Bo He, Andrés Garzón-Ruiz, Amparo Navarro, Teresa L. Chen, Matthew A. Kolaczkowski, Shizhen Feng, Lianjie Zhang, Christopher A. Anderson, Junwu Chen,\* and Yi Liu\**

Three series of low-bandgap polymers based on a novel quinoidal *para*-azaquinodimethane (*p*-AQM) unit are devised and synthesized, enabling an in-depth study of the impact of structural factors such as polymer main chain, branching point of the side chain, and the length of the branch chains on the thin film morphologies and charge transport properties. Morphological studies reveal that the polymers composed of larger repeating units exhibit a stronger tendency to form edge-on lamella. On the other hand, altering the side chain structures of polymers with the same main chain configuration indicates that the branching point position has a more deterministic impact than the branch chain length on the interchain interactions and the crystallite orientation. These results demonstrate a compound odd-even effect of the branching point on the chain packing and morphology, which correlates well with the corresponding field effect transistor performances. The polymer with the branching point at the fourth carbon displays the highest charge carrier mobility over 1.0 cm$^2$ V$^{-1}$ s$^{-1}$, concurrent with a bimodal texture. This study provides a comprehensive description of the correlations between polymer structures, thin film morphology, and device performances, providing a clear path to desirable bimodal thin film texture for charge transport.

## 1. Introduction

Conjugated polymers have received great attention for their application in organic field effect transistors (OFETs),[1] organic photovoltaics (OPVs),[2] and other area of flexible electronics.[3] In order to tune the overall optoelectronic properties of conjugated polymers and their device performances, critical materials design considerations have been undertaken to address both intrachain electron delocalization and interchain packing.[4] Intrachain control is often implemented by the use of properly chosen electronic building blocks to adjust the molecular orbital levels and polymer main chain conformation. On the other hand, interchain packing, which governs ordering, crystallinity, and orientation in thin films, is strongly dependent on both the conformation of the polymer main chain and the configuration of side chains.[2d,5a,b–e]

Dr. X. Liu, Dr. B. He, T. L. Chen, M. A. Kolaczkowski, C. A. Anderson, Dr. Y. Liu
The Molecular Foundry
Lawrence Berkeley National Laboratory
One Cyclotron Road, Berkeley, CA 94720, USA
E-mail: yliu@lbl.gov

Dr. X. Liu, S. Feng, Dr. L. Zhang, Prof. J. Chen
Institute of Polymer Optoelectronic Materials and Devices
State Key Laboratory of Luminescent Materials and Devices
South China University of Technology
Guangzhou 510640, P. R. China
E-mail: psjwchen@scut.edu.cn

Dr. B. He, Dr. Y. Liu
Materials Sciences Division
Lawrence Berkeley National Laboratory
One Cyclotron Road, Berkeley, CA 94720, USA

Dr. A. Garzón-Ruiz
Department of Physical Chemistry
Faculty of Pharmacy
Universidad de Castilla-La Mancha
Cronista Francisco Ballesteros Gómez, 1, E02071 Albacete, Spain

Dr. A. Navarro
Department of Physical and Analytical Chemistry
Faculty of Experimental Sciences
Universidad de Jaén
Campus Las Lagunillas E23071, Jaén, Spain

M. A. Kolaczkowski, C. A. Anderson
Department of Chemistry
University of California, Berkeley
Berkeley, CA 94720, USA

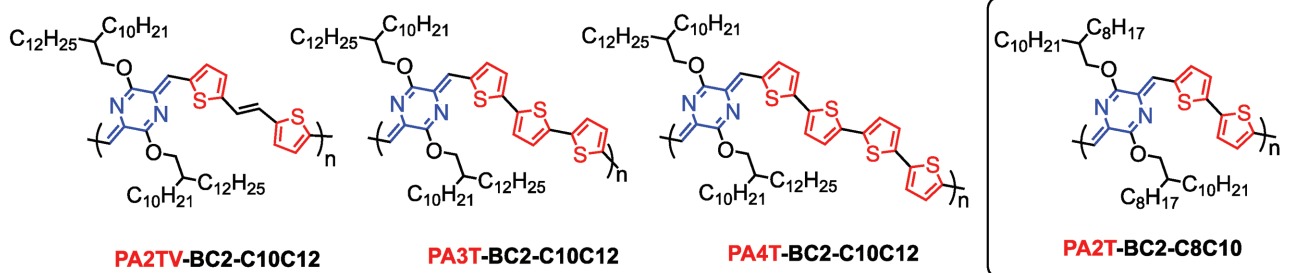The ORCID identification number(s) for the author(s) of this article can be found under https://doi.org/10.1002/adfm.201801874.

In parallel to the great endeavor in modifying the polymer main chain structures to tune the overall electronic properties, many recent efforts have been devoted to understanding the influence of side chains on polymer packing in the thin films.[5c,6a,b,c] The side chains are crucial structural units of conjugated polymers, nominally introduced for solution processibility considerations rather than for energetic contributions. Branched alkyl and alkoxy side chains are the most commonly used solubilizing groups, the branching point and length of which have been proven vital in determining key morphological parameters and crystallinity of the resulting thin films. Several recent studies have elucidated that shifting the branching point position of the alkyl chains can lead to dramatic changes of charge carrier mobilities in OFETs.[7] Such studies are more systematically carried out toward isoindigo-[7a] and diketopyrrolopyrrole-based polymers,[8] the two representative classes of high mobility conjugated polymers. The preferred side chains are however largely dependent on the exact polymer systems
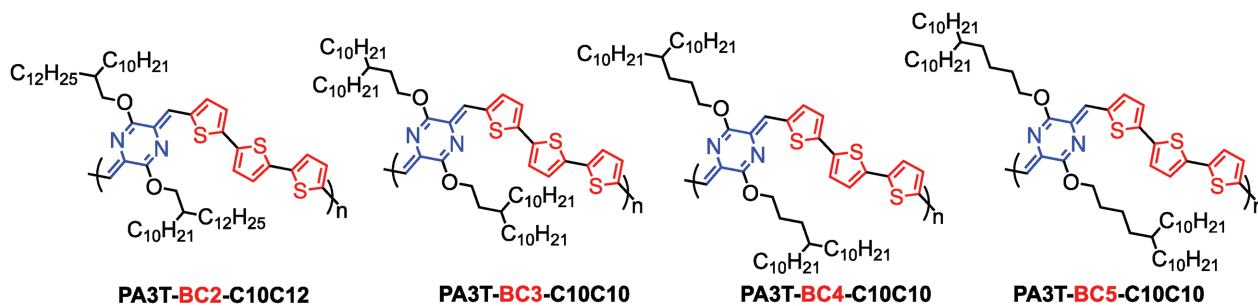
and may not be generalized to other polymers with different main chain structures.

In the course of designing low-bandgap conjugated polymers, we have discovered that *para*-azaquinodimethane (*p*-AQM) is a potent quinoidal building block attainable in a few simple steps.[9] The succinct synthesis warrants facile access to a series of conjugated polymers by copolymerizing *p*-AQM with unsubstituted bithiophene (2T), terthiophene (3T), and quarterthiophene (4T) units, the bandgaps of which follow an opposite trend to the conventional donor–acceptor polymers as a result of the unique quinoidal characteristics of *p*-AQM. Among these polymers, the 3T-based polymer bearing 2-decyltetradecoxy side chains (**Scheme 1**) show the highest field effect charge carrier mobility over 0.5 cm$^2$ V$^{-1}$ s$^{-1}$, which is very promising compared to other high-performing quinoidal polymers.[10] Despite these initial studies primarily focusing on tuning electronic structures, the full potential of such class of materials as high mobility semiconductors remains unraveled, which calls for a comprehensive
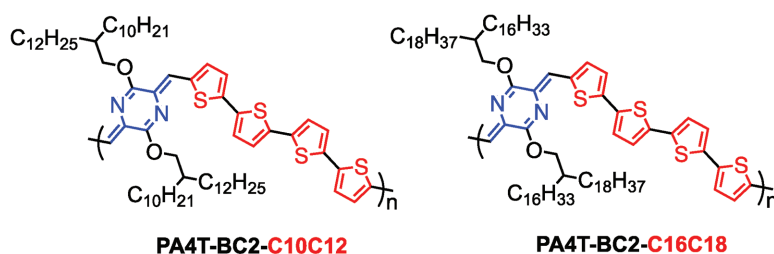
*(a) Series 1: polymers with different main chain structures*



PA2TV-BC2-C10C12        PA3T-BC2-C10C12        PA4T-BC2-C10C12        PA2T-BC2-C8C10

*(b) Series 2: polymers containing side chains with varying branching point*



PA3T-BC2-C10C12        PA3T-BC3-C10C10        PA3T-BC4-C10C10        PA3T-BC5-C10C10

*(c) Series 3: polymers containing side chains with different branch lengths*



PA4T-BC2-C10C12        PA4T-BC2-C16C18

**Scheme 1.** List of *p*-AQM-containing conjugated polymers grouped into three series

study of the main chain effect and side chain effect. Herein, we have systematically varied the main chain structure, the branching point, and the length of the side chains. Detailed studies of their thin film morphologies using grazing incidence wide-angle X-ray scattering (GIWAXS) reveal strong correlation between the crystallite orientation and both the main chain and the side chain structures. In particular, a compound "odd-even" effect concerning the branching point of the side chains has been observed and understood by computational modeling. Charge transport studies show that the side chain engineering results in enhanced field effect mobilities over 1.0 cm$^2$ V$^{-1}$ s$^{-1}$ in thin films featuring bimodal crystallite orientations. Such studies provide unique insight into the relationship between polymer structures, thin film morphologies, and charge transport properties that will help guide the future design of conjugated polymers.

## 2. Results and Discussion

Three groups of polymers are devised to highlight different structural variations. The first series are polymers with the same 2-decyltetradecoxy side chain but different main chain structures featuring the comonomers of p-AQM and thienylvinylthiophene (2TV), terthiophene (3T), and quarterthiophene (4T) units (Scheme 1a). A nomenclature PAnT(V)-BCn-CxCy is adopted to underline the different composition of the main chain aromatic structure, the position of the branching point, and the number of carbon on each branch. Accordingly, the corresponding polymers are named as PA2TV-BC2-C10C12, PA3T-BC2-C10C12, and PA4T-BC2-C10C12, respectively. A bithiophene (2T) polymer with slightly shorter branched side chains, PA2T-BC2-C8C10, was also included in the series for comparison (boxed structure in Scheme 1a).

The second and third series are polymers with the same main chain structure but bearing different side chains, with the former featuring systematically shifted branching points (Scheme 1b) and the latter featuring significantly different branch chain lengths (Scheme 1c). For the second series, we focus on the conjugated polymers containing PA3T repeating units in the main chain since it has exhibited higher carrier mobility than other oligothiophene-based polymers.[9] Alkoxy side chains with systematically shifted branching point, such as 3-decyltridecoxy,
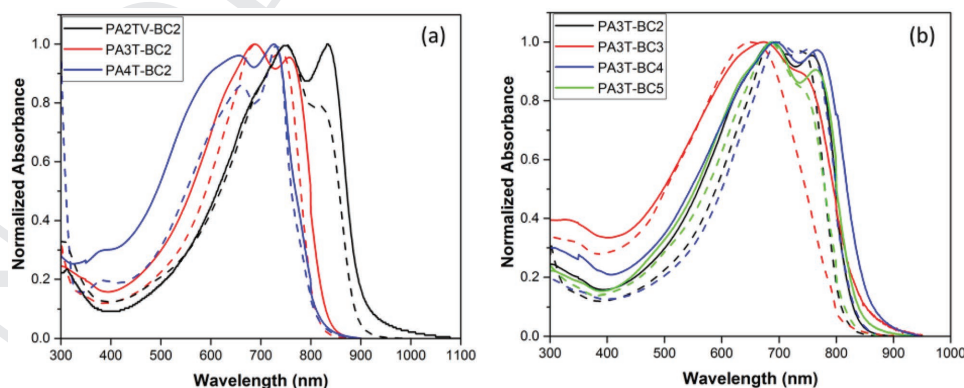
4-decyltetradecoxy, and 5-decylpentadecoxy, were introduced to give the series PA3T-BCn-C10C10, with n being 3, 4, and 5 to denote the different position of branching point based on number of carbons, respectively. The polymer PA3T-BC2-C10C12, which is listed in Series 1 and has a branching point at C2 position, is included in Series 2 for comparison despite that the two branched alkyl chains are nonequivalent. Series 3 enlists two conjugated PA4T-BC2 polymers bearing side chains with significantly varied lengths, namely, PA4T-BC2-C10C12 (also listed in Series 1) and PA4T-BC2-C16C18, respectively.
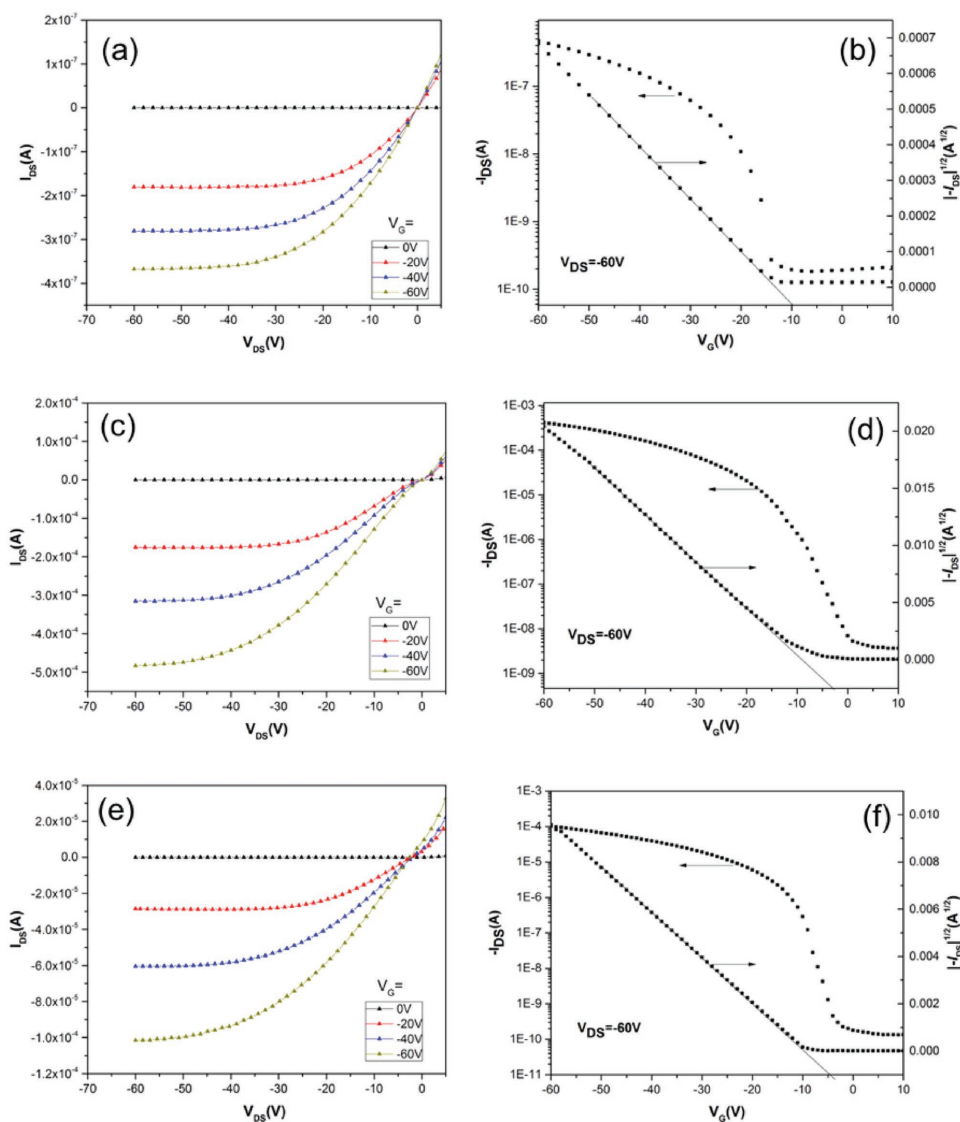
### 2.1. Polymer Synthesis

The synthesis of p-AQM monomers and all the polymers follows a modular synthetic protocol[9] and is included in the Supporting Information. Briefly, the p-AQM monomers **S2a-e** were furnished by alkylation of the diarylidene piperazinedione **S1**[9] with the corresponding alkyl bromides. Pd-catalyzed cross-coupling polymerization between **S2a-d** and the corresponding comonomers afforded the desired polymers. PA2T-BC2-C8C10, PA3T-BC2-C10C12, and PA4T-BC2-C10C12 in Series 1 were synthesized previously.[9] The solubility of polymers decreases as the main chain repeating unit becomes larger, as observed for the Series 1 polymers, and increases as the side chain becomes longer for the Series 3 polymers. The solubility and molecular weight of the PA3T-BCn polymers in series 2 show a correlation to an odd-even effect of the branching point. The number-averaged molecular weights of PA3T-BC3-C10C10 and PA3T-BC5-C10C10 are around 10 000, while these of PA3T-BC2-C10C12 and PA3T-BC4-C10C10 are over 26 000. Despite the higher molecular weight of the latter two polymers, they exhibit considerably higher solubility than PA3T-BC3-C10C10 and PA3T-BC5-C10C10. PA3T-BC2-C10C12 and PA3T-BC4-C10C10 are readily soluble in solvents such as chloroform and chlorobenzene at room temperature, while the latter two are difficult to dissolve even at elevated temperature.

### 2.2. Optical and Electrochemical Properties

The UV–vis absorption spectra of these polymers are indicative of the low-bandgap characteristics (**Figure 1** and



**Figure 1.** Normalized solution (in chlorobenzene, dashed lines) and thin film (solid lines) absorption spectra of a) the PAnT(V)-BC2 polymers and b) the PA3T-BCn (n = 2–5) polymers.

**Figure 2.** Typical output and transfer characteristics of OFETs based on a,b) PA3T-BC3-C10C10, c,d) PA3T-BC4-C10C10, and e,f) PA3T-BC5-C10C10. (a), (c), and (e) Output curves; (b), (d), and (f) transfer curves.

**Table 1**). All polymers except PA3T-BC3-C10C10 show a dual-band absorption in chlorobenzene solution. The dual-band feature, corresponding to the 0-0 and 0-1 transitions, is indicative of preaggregated states in the solutions of these polymers. A comparison of the three Series 1 polymers with the same side chains shows that the bandgap increases as the number of thiophene increases, consistent with previous findings (Figure 1a). The two polymers in Series 3 show nearly identical absorption in both solution and the thin film, suggesting that different branch chain length has little impact on the optical properties (Figure S1, Supporting Information). For the Series 2 polymers, the 0-0 peak of PA3T-BC4-C10C10 is at the longest wavelength. In contrast, PA3T-BC3-C10C10 has no noticeable aggregation peak in its absorption spectrum, and also its absorption maximum is considerably blueshifted even when compared to PA3T-BC2-C10C12. The trend of the solution optical bandgap changes is again in accordance

with an odd-even effect of the branching point. The abnormal behavior of PA3T-BC3-C10C10 may suggest decreased coplanarity and conjugation of the polymer main chain due to the increased steric hindrance imposed by the specific branching pattern, which is discussed in further details later. A new shoulder peak arises in the thin film absorption spectrum of PA3T-BC3-C10C10, suggesting reinforced coplanarity and stronger chain aggregation in the solid state. The dual band absorption feature for all other polymers is preserved in the corresponding thin film absorption spectra, together with slight redshift of the 0-0 transition peaks, also consistent with enhanced coplanarity and stacking in the solid state. Overall, the optical bandgaps of these polymers are strongly dependent on the main chain structure but much less so on the side chains, as can be seen from the apparent shift of 0-0 transition peaks from 1.53 to 1.36 eV in the spectra of Series 1 polymers, while these for the Series 2 polymers

**ADVANCED
SCIENCE NEWS**

www.advancedsciencenews.com

**ADVANCED
FUNCTIONAL
MATERIALS**

www.afm-journal.de

**Table 1.** Summary of the optical and electrochemical properties and frontier orbital energies.

| Polymer | UV–vis | | | | | | Frontier orbital energies | |
|---|---|---|---|---|---|---|---|---|
| | Solution[a] | | | Film | | | | |
| | $\lambda_{max}$ [nm] | $\lambda_{onset}$ [nm] | $E_g^{opt}$ [eV] | $\lambda_{max}$ [nm] | $\lambda_{onset}$ [nm] | $E_g^{opt}$ [eV] | HOMO[b] [eV] | LUMO[c] [eV] |
| PA2TV-BC2-C10C12 | 824 | 896 | 1.38 | 834 | 910 | 1.36 | −5.0 | −3.6 |
| PA3T-BC2-C10C12 | 742 | 810 | 1.53 | 758 | 832 | 1.49 | −5.0 | −3.5 |
| PA4T-BC2-C10C12 | 731 | 805 | 1.54 | 731 | 810 | 1.53 | −5.1 | −3.5 |
| PA3T-BC3-C10C10 | 655 | 802 | 1.55 | 745 | 836 | 1.48 | −4.9 | −3.4 |
| PA3T-BC4-C10C10 | 752 | 832 | 1.49 | 766 | 858 | 1.45 | −4.9 | −3.4 |
| PA3T-BC5-C10C10 | 748 | 809 | 1.53 | 763 | 841 | 1.47 | −4.9 | −3.4 |
| PA4T-BC2-C16C18 | 726 | 805 | 1.54 | 726 | 820 | 1.51 | −5.1 | −3.5 |

[a]Measured in chlorobenzene; [b]Calculated using $E_{HOMO} = -(4.8-E_{ox})$ eV. The $E_{ox}$ was measured by cyclic voltammetry using conventional three-electrode setup at a scan rate of 100 mV s$^{-1}$; [c]Calculated using the corresponding $E_{HOMO}$ and $E_g^{opt}$.

are within 1.45 and 1.49 eV based on the absorption edges of the respective thin films. Approximate frontier orbital energy levels[11] of the polymers were estimated from cyclic voltammetry (Figure S2, Supporting Information) and optical gaps and summarized in Table 1. Not unexpectedly, the highest occupied molecular orbital (HOMO) and lowest unoccupied molecular orbital (LUMO) energy levels for the Series 2 polymers vary only slightly in the range between −5.0 and −4.9 eV and between −3.5 and −3.4 eV, respectively.

### 2.3. Thin Film FET Measurements

Charge transport properties of all the polymers were evaluated in thin film field effect transistors, using the bottom gate/top contact OFET configuration with octadecyltrichlorosilane (OTS)-modified SiO$_2$ as the dielectric layer. Gold (Au) was used as the source/drain electrodes, and scratched n-doped Si was used as the gate electrode. The devices were fabricated using as-cast thin films or those thermally annealed at 200 or 225 °C. All the devices displayed distinct p-type transporting behavior. PA2TV-BC2-C10C12 had a hole mobility ($\mu$) of $3.9 \times 10^{-3}$ cm$^2$ V$^{-1}$ s$^{-1}$, which was lower than that of the other polymers in Series 1 that were reported previously (Table S1, Supporting Information).[9] The two polymers in Series 3 displayed very comparable mobilities around $8.0 \times 10^{-2}$ cm$^2$ V$^{-1}$ s$^{-1}$, indicating that the branch chain length variation has little impact on the charge transport properties (Table S1, Supporting Information).

For the Series 2 polymers, PA3T-BC3-C10C10 displayed the lowest hole mobility among all four polymers, with a maximum and average mobility of $7.0 \times 10^{-3}$ and $5.0 \times 10^{-3}$ cm$^2$ V$^{-1}$ s$^{-1}$, respectively (**Table 2**). This value is nearly two orders lower than that of the previously reported PA3T-BC2-C10C12 (0.54 cm$^2$ V$^{-1}$ s$^{-1}$). PA3T-BC5-C10C10 showed a comparable mobility to PA3T-BC2-C10C12 of 0.32 cm$^2$ V$^{-1}$ s$^{-1}$. PA3T-BC4-C10C10 displayed the highest transporting property among the series, with the mobility up to 1.05 cm$^2$ V$^{-1}$ s$^{-1}$ and an average mobility of 0.92 cm$^2$ V$^{-1}$ s$^{-1}$. The overall trend of mobilities follows an odd-even relationship with respect to the branching positions. Devices based on PA3T-BC4-C10C10 and PA3T-BC5-C10C10 also feature low threshold voltages, which suggest low charge trapping sites in the active layer.

### 2.4. Morphological Studies

GIWAXS measurements were conducted to probe molecular packing within the spun-cast films. Thin films were either as cast or annealed at 200 °C for 30 min unless stated otherwise before being subjected to synchrotron X-ray studies. Greater details regarding the molecular packing and orientation are revealed from the comparative studies of the different series, as itemized below
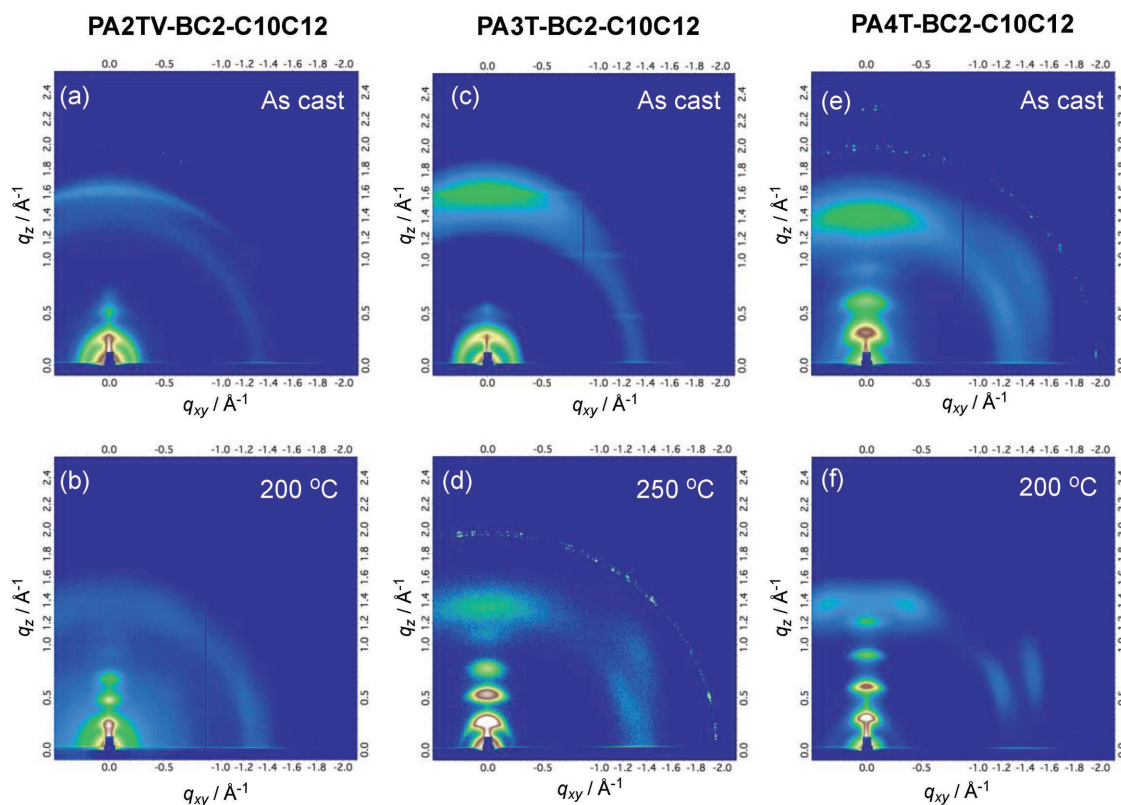
#### 2.4.1. The Main Chain Effect

Studies of the Series 1 polymers revealed that for the polymers bearing the same side chain, as the size of the repeating unit becomes larger, the crystallites tend to adopt an edge-on orientation over the face-on one. This can be seen from the textures of both the room temperature and the annealed thin films of the polymers. As shown in **Figure 3**, the as-cast thin films of PA2TV-BC2-C10C12 and PA3T-BC2-C10C12 have a bimodal texture, showing the presence of both face-on and edge-on lamellas, while PA4T-BC2-C10C12 has a pure edge-on orientation. The face-on component decreases upon thermal annealing, and completely disappears at 200 °C for PA2TV-BC2-C10C12 and at 250 °C

**Table 2.** Summary of OFET characteristics of Series 2 polymers.

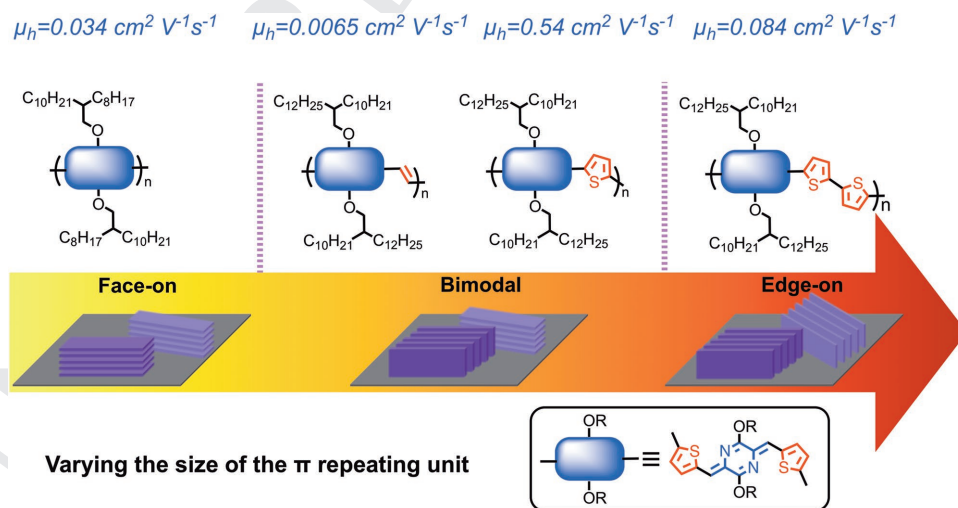| Polymers | $T_{annealing}$ [°C] | $\mu_h^{avg,a}$ [cm$^2$ V$^{-1}$ s$^{-1}$] | $\mu_h^{max,b}$ [cm$^2$ V$^{-1}$ s$^{-1}$] | $V_{th}$ [V] | $I_{On}/I_{Off}$ |
|---|---|---|---|---|---|
| PA3T-BC2-C10C12[c] | 200 | 0.47 | 0.54 | −14 | $5 \times 10^5$ |
| PA3T-BC3-C10C10 | 200 | 0.005 | 0.007 | −10 | $3 \times 10^3$ |
| PA3T-BC4-C10C10 | 225 | 0.92 | 1.05 | −3 | $2 \times 10^5$ |
| PA3T-BC5-C10C10 | 225 | 0.26 | 0.32 | −4 | $8 \times 10^5$ |

[a]Average mobility; [b]Maximum mobility; [c]Reported previously.

**Figure 3.** GIWAXS patterns of thin films of a,b) PA2TV-BC2-C10C12, c,d) PA3T-BC2-C10C12, and e,f) PA4T-BC2-C10C12. (a), (c), and (e): as-cast; (b) and (f): 200 °C; (d) 250 °C.

for PA3T-BC2-C10C12, respectively. This is consistent with the literature report that polymers with lower side chain density have a stronger tendency of forming edge-on oriented crystallites due to tighter packing between lamellas.[12] Tighter packing is clearly observed in this series, as the interlamella distance ($d_{100}$) for the thermally annealed polymers decreases from 2.63 nm for PA2TV-BC2-C10C12, to 2.23 nm for PA3T-BC2-C10C12 and to 2.05 nm for PA4T-BC2-C10C12. It is worth noting that the polymer PA2T-BC2-C8C10 with an even smaller main chain repeating unit (A2T) than that of PA2TV-BC2-C10C12,[9] despite slightly shorter side chains, adopts a pure face-on orientation at both room temperature and after thermal annealing (Figure S3, Supporting Information). The solid-state packing behavior complements the range of orientation preferences that changes progressively from face-on to bimodal to pure edge-on as the side chain density decreases, as illustrated in **Figure 4**.
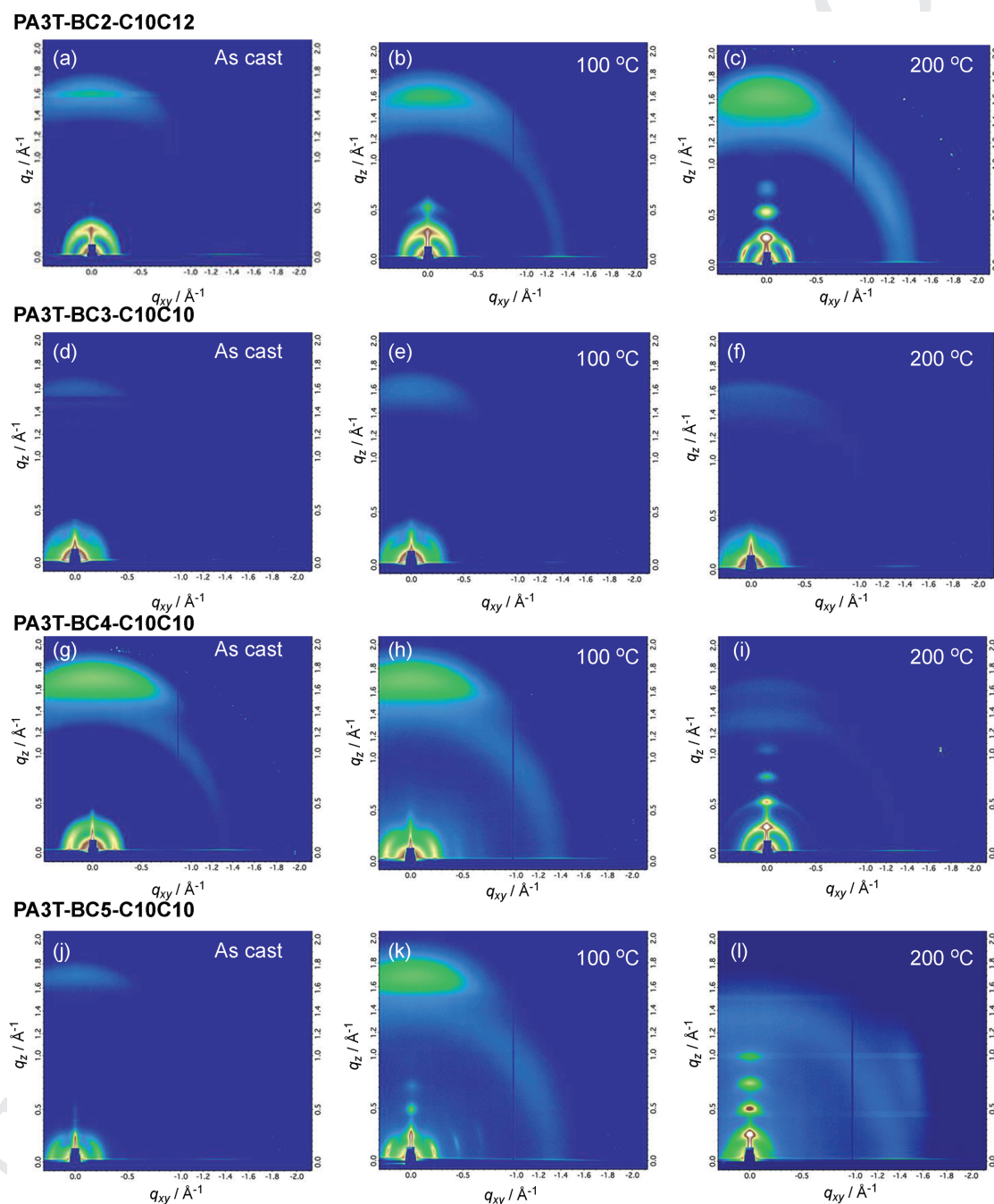


**Figure 4.** Summary of the dependence of crystallite orientations on the main chain structure.

**ADVANCED
SCIENCE NEWS**
www.advancedsciencenews.com

**ADVANCED
FUNCTIONAL
MATERIALS**
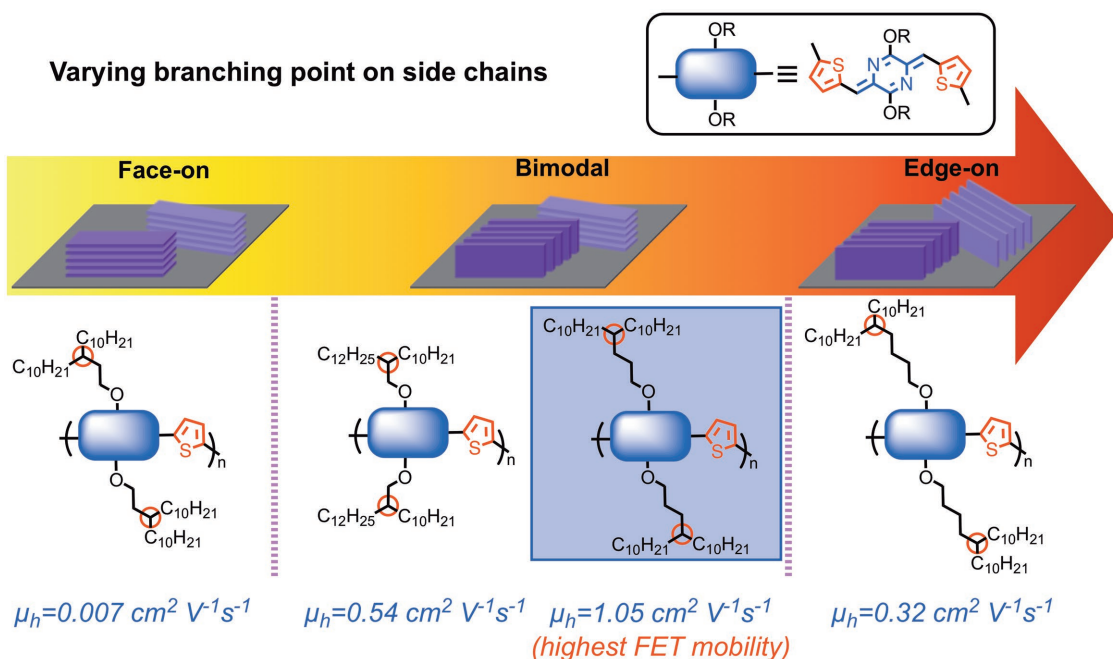www.afm-journal.de

### 2.4.2. Branching Side Chain Effect

Several notable trends could be summarized from the GIWAXS studies of the Series 2 polymers.

(1) Face-on orientation is observed in the as-cast films of all the PA3T polymers, and the interlamellar spacing in the face-on crystallites increases monotonically as the side chain length becomes larger. In the case of PA3T-BC2-C10C12, it coexists with a significant fraction of edge-on orientation (**Figure 5**).

The interlamellar distances of the face-on and edge-on crystallites are 2.53 and 2.23 nm, respectively. In contrast, for the polymers with branching point more than two carbons away from the main chain, they all adopt a pure face-on orientation, with PA3T-BC3-C10C10 being the least crystalline. The interlamellar $d$-spacings of the face-on crystallites are 2.27, 2.60, and 2.71 nm for PA3T-BC3-C10C10, PA3T-BC4-C10C10, and PA3T-BC5-C10C10, respectively. It should be noted that the side chains in PA3T-BC2-C10C12 are composed of two alkyl branches with two carbon differences,

**PA3T-BC2-C10C12**

**PA3T-BC3-C10C10**

**PA3T-BC4-C10C10**

**PA3T-BC5-C10C10**



**Figure 5.** GIWAXS patterns of thin films of a–c) PA3T-BC2-C10C12, d–f) PA3T-BC3-C10C10, g–i) PA3T-BC4-C10C10, and j–l) PA3T-BC5-C10C10. (a), (d), (g), and (j): as-cast; (b), (e), (h), and (k): 100 °C; (c), (f), (i), and (l): 200 °C.

**Figure 6.** Summary of the dependence of crystallite orientations on the branching point of the side chains.

and the overall length of the side chains should be close to that of P3AT-BC4-C10C10. Indeed, the corresponding face-on interlamellar spacing of PA3T-BC2-C10C12 (2.53 nm) is larger than that of PA3T-BC3-C10C10 (2.27 nm) and close to that of PA3T-BC4-C10C10 (2.60 nm).

(2) Edge-on is the thermodynamically more preferred orientation for all the PA3T polymers except PA3T-BC3-C10C10. As can be seen from Figure 5, PA3T-BC3-C10C10 thin film retains its face-on orientation with low crystallinity after thermal annealing, with no changes of the interchain *d*-spacing. This is in contrast to all other polymer films that show clear transition from face-on to edge-on upon annealing to 100 and 200 °C. A mixed texture is observed in the annealed thin films of PA3T-BC2-C10C12 and PA3T-BC4-C10C10. The edge-on oriented crystallites are evidenced by the strong out-of-plane ($n$00) peaks ($n$ up to 4) while the out-of-plane (001) peak indicates the coexisted face-on crystallites. In the case of PA3T-BC5-C10C10, the strong out-of-plane ($n$00) peaks ($n$ up to 4) together with the absence of out-of-plane (001) peak clearly indicate a pure edge-on phase and the absence of face-on component. For the 200 °C annealed samples, the interlamellar *d*-spacings for edge-on crystallites are 2.32, 2.34, and 2.49 nm for PA3T-BC2-C10C12, PA3T-BC4-C10C10, and PA3T-BC5-C10C10, respectively (no edge-on for PA3T-BC3). On the other hand, the interlamellar *d*-spacings for face-on crystallites, which remain nearly constant upon annealing, are 2.53, 2.24, and 2.58 nm for PA3T-BC2-C10C12, PA3T-BC3-C10C10, and PA3T-BC4-C10C10 (no face-on for annealed PA3T-BC5). In both orientations, the interlamellar *d*-spacings increase as the length of the side chains becomes larger. In all cases when both face-on and edge-on oriented crystallites are present, the interlamellar *d*-spacing of the face-on is always larger than that of the edge-on crystallites, which is indicative of tighter chain packing in the latter.
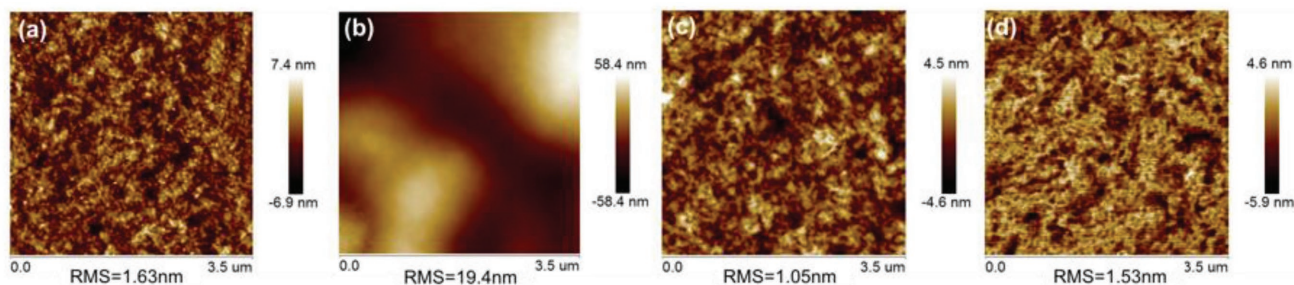
The transition from face-on in PA3T-BC3-C10C10 to bimodal in PA3T-BC4-C10C10, and to edge-on in PA3T-BC5-C10C10 in thermally treated thin films indicates a preference for edge-on conformation as the branching point moves further away from the polymer main chain. A comparison of the thin films of PA3T-BC$n$-C10C10 ($n$ = 3–5) annealed at 100 °C shows that at this intermediate temperature, both PA3T-BC3-C10C10 and P3AT-BC4-C10C10 remain face-on, while PA3T-BC5-C10C10 clearly has developed strong edge-on texture (Figure 5). Counting PA3T-BC2-C10H12 in the series, the overall trend observes that, with the exception of PA3T-BC3, the farther away the branching point is from the polymer main chain, the more edge-on it becomes upon thermal annealing, as illustrated in **Figure 6**.

Tapping-mode atomic force microscopic (AFM) studies of the thermally annealed thin films of the Series 2 polymers revealed additional information about the surface morphology and roughness (**Figure 7**). PA3T-BC3-C10C10 has a very rough surface with a root-mean-square (RMS) roughness of 19.4 nm. This large roughness is in accordance with its low solubility and inferior mobility. On the other hand, PA3T-BC4-C10C10 thin film is very smooth with a roughness of only 1.05 nm and a fibril network structure. In the case of PA3T-BC5-C10C10, it has good film forming ability despite its low solubility, giving rise to a similar fibril network structure with slight larger roughness of 1.53 nm. These features are comparable to PA3T-BC2-C10C12, which also exhibits a fibril network with a roughness of 1.63 nm.

### 2.4.3. Side Chain Length Effect

As shown in Figure S4 (Supporting Information), both polymers in the Series 3 behave very similarly and adopt an edge-on

**Figure 7.** AFM images of the thin films of a) PA3T-BC2-C10C12, b) PA3T-BC3-C10C10, c) PA3T-BC4-C10C10, and d) PA3T-BC5-C10C10 after annealing at 200 °C (3.5 μm × 3.5 μm).

orientation throughout the thermal treatment. The interlamella distance remains constant during the thermal annealing while small changes of the diffraction pattern were observed, which indicates more ordered side chain organization upon equilibrium. More notably, the interlamella distance varies only slightly from 2.05 nm for PA4T-BC2-C10C12 to 2.08 nm for PA4T-BC2-C16C18. Compared to the significant disparity of the branch chain lengths that differ by six carbon atoms, this variation is very insignificant, which suggests less steric crowdedness between lamellas as a result of more void space created by the larger π-surface of PA4T. The very similar interlamella packing between the two polymers is also consistent with their comparable device behavior.

## 2.5. Correlations between Mobility and Morphology

The study of the Series 1 polymer indicates that the thermally annealed PA3T polymer has the highest mobility, the thin film of which displays a bimodal texture. On the other hand, comparison of the Series 3 polymer suggests that side chain length has minimal effect on the film morphology and related charge transport. The behavior of Series 2 polymers further indicates that the side chain modulated fluctuation of mobilities of PA3T polymers correlates well with the observed morphological trend, which bodes well for the importance of bimodal orientation for facile charge transport. The lowest mobility PA3T-BC3-C10C10 maintains a face-on orientation throughout the annealing process. All three other PA3T polymers prefer a face-on orientation in the as-cast thin films but display different phase purity upon thermal annealing. PA3T-BC2-C10C12 remains a mixed face-on and edge-on texture throughout the annealing (up to 200 °C). PA3T-BC4-C10C10 transitions from a face-on orientation to a mixed bimodal texture upon annealing to give the highest mobility. Moving the branching point further away from the polymer main chain led to pure edge-on lamellar stacking after annealing, concomitant with a lower charge transport mobility for PA3T-BC5-C10C10. Such correlations provide consistent experimental evidences that highlight the benefit of developing bimodal orientations in the thin films, which facilitate the formation of an effective 3D conduction network for more efficient charge transport.[13]
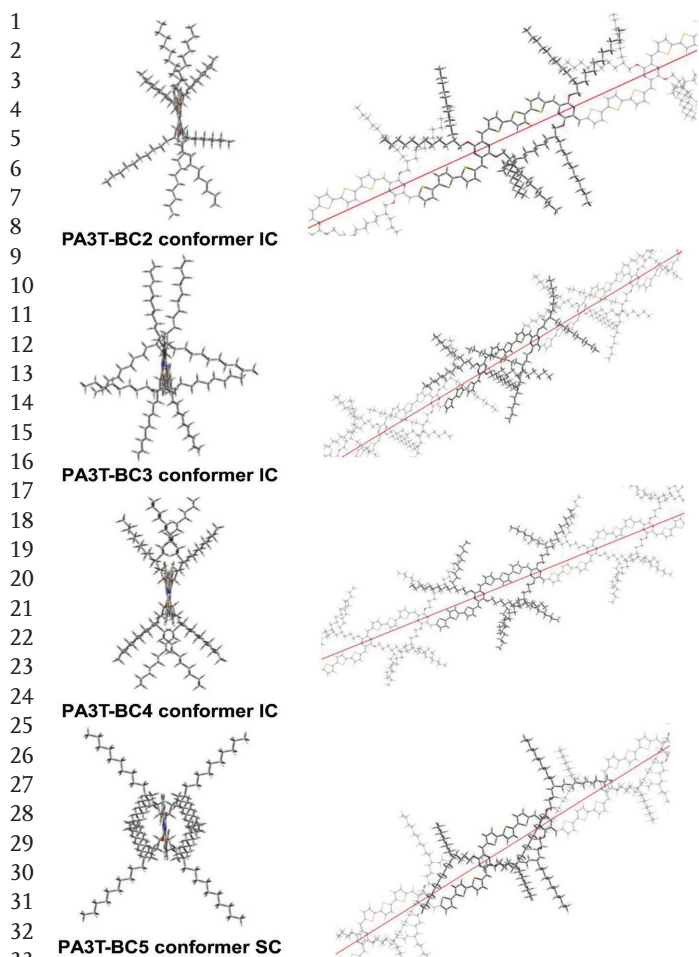
When taking molecular weight into consideration, we note that there lacks a direct correlation between molecular weight and charge carrier mobility. Polymer PA3T-BC4-C10C10 has a significantly lower $M_n$ than PA3T-BC2-C10C12, yet the mobility of the former is much higher. On the other hand, polymers PA3T-BC3-C10C10 and PA3T-BC5-C10C10 have comparable $M_n$ yet the former has a much lower mobility. These results suggest that the charge transport mobility of such series of polymers is less contingent on molecular weight but more so on aggregation order and morphology, which is consistent with previous findings.[14]

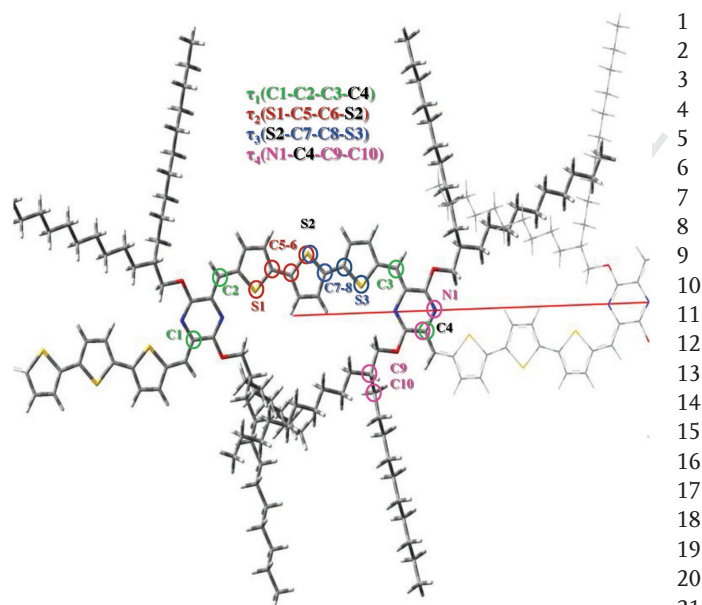## 2.6. Modeling of the Branching Chain Effect

In the Series 2 polymers, PA3T-BC3-C10C10 appears as an outliner that behaves differently from the rest, alluding to subtle steric factors that affect the chain packing behavior. More detailed DFT modeling of that series of polymer chains was thus conducted to provide more insight into the branching chain effect (see the Supporting Information for more detailed information on the previous conformational study of short oligomers as well as setting up of the starting structures for the modeling). **Figure 8** shows the most stable structures computed for the titled polymer chains for which two different starting conformations, generated by slight rotation of the prebranching point side chains, were employed as calculation starting point, that is, intercrossed (IC) and separated (SC) conformations (see the Supporting Information for more details).

In polymer PA3T-BC2, the short prebranching point side chains avoid significant steric hindrances between postbranching point chains. Hence, both the starting points SC and IC led to similar molecular conformations with close energies (see dihedral angles defined in **Figure 9** and relative energies shown in **Table 3**). The polymer main chain is not fully planar and the calculations yielded a value of 20° for the dihedral angle $|\tau_1|$. Dihedral angles, $|\tau_2|$ and $|\tau_3|$, between subsequent thiophene rings amount to 166°–177°. In general, similar conformations were observed for the rest of polymer chains studied here. Notably, the postbranching point chains of PA3T-BC2 are oriented out of the plane of the polymer main chain (Figure 8). In contrast, the postbranching point chains are oriented toward the cofacial area of the polymer main chain in both conformers of PA3T-BC3 (Figure 8). The change of orientation in the postbranching point chains is reflected in the values of the dihedral angles $|\tau_4|$ which are within 119°–130° for PA3T-BC2 and 17°–51° for PA3T-BC3. The orientation of the postbranching point chains in PA3T-BC3 can hinder the π-stacking interactions between neighbor polymer

**PA3T-BC2 conformer IC**

**PA3T-BC3 conformer IC**

**PA3T-BC4 conformer IC**

**PA3T-BC5 conformer SC**

**Figure 8.** Infinite polymer chains optimized for PA3T-BC2 (conformer IC), PA3T-BC3 (conformer IC), PA3T-BC4 (conformer IC), and PA3T-BC5 (conformer SC) at the B3LYP/3-21G* level of theory. The repeat unit is highlighted on the polymer chain. The translation vector of the periodic calculation is shown in red.



$\tau_1$(C1-C2-C3-C4)
$\tau_2$(S1-C5-C6-S2)
$\tau_3$(S2-C7-C8-S3)
$\tau_4$(N1-C4-C9-C10)

**Figure 9.** Repeating unit of a polymer chain showing the dihedral angles selected to analyze the molecular structure of the studied compounds. The values calculated for these angles are collected in Table 3.

chains, reducing the charge-hopping-based carrier transport mobility. In the bulk polymer, postbranching point chains generally can fold to accommodate the 3D structure. In the case of PA3T-BC3, however, the branching point (the zone with larger density of atoms of the side chain) is near the polymer main chain and significant steric hindrance can always be expected. The branch chains in PA3T-BC4 behave similarly as these in PA3T-BC2, with the postbranching point chains orienting out of the plane of the polymer main chains as indicated by the large dihedral angle ($|\tau_4| = 109°–141°$), from which reduced steric interactions between neighbor polymer chains are expected (Figure 8). Structural conformations calculated for PA3T-BC4 and PA3T-BC3 and their implication on the interchain interactions are consistent with the highest and lowest charge mobilities observed for these compounds, respectively. In the case of PA3T-BC5, the postbranching point chains are again oriented toward the polymer main chain, as in the case of PA3T-BC3, however the branching point is further away from the polymer chain than for the PA3T-BC3. As shown in Figure 8, the side chains of PA3T-BC5 could induce certain hindrance in between polymer main chains, however this steric effect is alleviated by the distant position of the branching point from the polymer main chain that allows the folding of the side chains. The polymer main chain of PA3T-BC5 is also the most planar of the series on the basis of $|\tau_{1–3}|$ values since the large separation of the branching point reduces the steric effect on the polymer chain. The computation results outline a compound odd-even effect: at odd or even branching point, the postbranching point chains are oriented toward or away from the polymer chain. In the former cases, the steric hindrance is disruptive to interchain packing. However, as the branching point is further moved away, the steric effect is alleviated and becomes less disruptive. PA3T-BC3 thus experiences the most hindrance among all and is the least well-packed in the thin film.

## 3. Conclusion

We have carried out a comprehensive study on the structure–property relationships of several low-bandgap polymers based on

**Table 3.** Values calculated at the B3LYP/3-21G* level of theory for the dihedral angles (in degrees) shown in Figure 9. These angles were computed for infinite polymer chains with C10 side chains beyond the branching point. $E_R$ (in kcal mol$^{-1}$) is the relative energy between the conformer IC (intercrossed chains) and the conformer SC (separated chains) for each polymer and calculation method ($E_R = 0$ corresponds to the most energetically stable conformer).

| Polymer | Conformer IC | | | | | Conformer SC | | | | |
|---|---|---|---|---|---|---|---|---|---|---|
| | $E_R$ | $|\tau_1|$ | $|\tau_2|$ | $|\tau_3|$ | $|\tau_4|$ | $E_R$ | $|\tau_1|$ | $|\tau_2|$ | $|\tau_3|$ | $|\tau_4|$ |
| BC2 | 0.00 | 20 | 166 | 177 | 119–130 | 0.21 | 20 | 167 | 176 | 125–127 |
| BC3 | 0.00 | 4 | 178 | 175 | 17–45 | 1.94 | 22 | 167 | 174 | 30–51 |
| BC4 | 0.00 | 20 | 171 | 171 | 121–132 | 2.65 | 17 | 172 | 172 | 109–141 |
| BC5 | – | – | – | – | – | – | 0.9 | 172 | 168 | 29–35 |

a novel *p*-AQM quinoidal unit, with further insight provided by detailed theoretical modeling. This study was implemented by devising several series of polymers that allow for independent investigation of the main chain effect and two side chain effects involving both the branching point and the chain length. In the PA*n*T-BC2 series, the polymers bearing the same 2-decyltetradecoxy side chains but with increasing size of the repeating unit in the polymer main chain have a stronger tendency to form edge-on oriented lamellas in the as-cast thin films. Upon thermal annealing, the face-on fraction is significantly reduced to give pure edge-on lamellas. For the PA3T-BC*n* (*n* = 3–5) series of polymers that consist of the same conjugated backbone but with systematically varied branched alkoxy side chains, the branching point of the side chains has a dramatic impact on the interchain interactions as well as the orientation of the crystallites on the substrate. A face-on orientation is observed in the as-cast thin films of all four PA3T polymers. Thermal annealing induces orientation transition from face-on to edge-on lamellas at different degrees, varying significantly across the differently branched polymers and is clearly related to the position of the branching point. When the branching point is moved away from the polymer main chain, the polymers are more inclined to transform from face-on to edge-on. Once beyond this point, the polymer chains have a stronger tendency to form edge-on lamellas with no face-on component. These results demonstrate a compound odd-even effect of the branching point, which amounts to a subtle steric effect as illustrated using detailed computational modeling. We have further shown that the length of the branch chains has little effect on the lamellar packing and the charge transport properties. Among these polymers, PA3T-BC4-C10C10, the one with branching point at the fourth carbon away from the main chain has the highest charge carrier mobility up to $1.05 \text{ cm}^2 \text{ V}^{-1} \text{ s}^{-1}$ in bottom gate, top-contact OFET devices.

The high carrier mobility highlights the great potential of *p*-AQM-based quinoidal conjugated polymers as novel high-performance organic semiconductors. On the other hand, the revealed correlation between the polymer structures (main chain structure, the side chain branching point, and the length of the branched chains), the thin film morphology, and device performances will serve as design principles to guide the development of high-performing organic semiconductors for anisotropic charge transport. The bimodal orientation in the highest performing polymer also highlights the importance to strike a balance between the two orientations:[15] while the edge-on oriented crystallites appear to be more favorable for in-plane charge transport, in semicrystalline polymer thin films there are abundant lattice defects and disordered aggregates that throttle the charge carrier movement. A mixed orientation is needed in order to form a 3D conduction network for optimal charge transport. While this study identifies discernible and consistent trends for predictive design and control of morphologies in conjugated polymer films, further studies should be directed toward revealing details of the interconnects between domains with different π-stacking orientations.[5b]

## Supporting Information

Supporting Information is available from the Wiley Online Library or from the author.

## Conflict of Interest

The authors declare no conflict of interest.

[1] a) C. Wang, H. Dong, W. Hu, Y. Liu, D. Zhu, *Chem. Rev.* **2011**, *112*, 2208; b) Y. Takeda, T. L. Andrew, J. M. Lobez, A. J. Mork, T. M. Swager, *Angew. Chem., Int. Ed.* **2012**, *51*, 9042; c) H. Dong, X. Fu, J. Liu, Z. Wang, W. Hu, *Adv. Mater.* **2013**, *25*, 6158; d) H. Li, F. S. Kim, G. Ren, S. A. Jenekhe, *J. Am. Chem. Soc.* **2013**, *135*, 14920; e) J. Mei, Y. Diao, A. L. Appleton, L. Fang, Z. Bao, *J. Am. Chem. Soc.* **2013**, *135*, 6724; f) Y. Zhao, Y. Guo, Y. Liu, *Adv. Mater.* **2013**, *25*, 5372; g) Z. Cai, H. Luo, P. Qi, J. Wang, G. Zhang, Z. Liu, D. Zhang, *Macromolecules* **2014**, *47*, 2899; h) T. Lei, X. Xia, J.-Y. Wang, C.-J. Liu, J. Pei, *J. Am. Chem. Soc.* **2014**, *136*, 2135.

[2] a) B. C. Thompson, J. M. J. Frechet, *Angew. Chem., Int. Ed.* **2008**, *47*, 58; b) J.-L. Brédas, J. E. Norton, J. Cornil, V. Coropceanu, *Acc. Chem. Res.* **2009**, *42*, 1691; c) Y.-J. Cheng, S.-H. Yang, C.-S. Hsu, *Chem. Rev.* **2009**, *109*, 5868; d) C. Cabanetos, A. El Labban, J. A. Bartelt, J. D. Douglas, W. R. Mateker, J. M. J. Fréchet, M. D. McGehee, P. M. Beaujuge, *J. Am. Chem. Soc.* **2013**, *135*, 4656; e) R. S. Kularatne, H. D. Magurudeniya, P. Sista, M. C. Biewer, M. C. Stefan, *J. Polym. Sci., Part A: Polym. Chem.* **2013**, *51*, 743; f) Y. Huang, E. J. Kramer, A. J. Heeger, G. C. Bazan, *Chem. Rev.* **2014**, *114*, 7006; g) Y. Li, K. Yao, H.-L. Yip, F.-Z. Ding, Y.-X. Xu, X. Li, Y. Chen, A. K. Y. Jen, *Adv. Funct. Mater.* **2014**, *24*, 3631; h) J. Warnan, C. Cabanetos, R. Bude, A. El Labban, L. Li, P. M. Beaujuge, *Chem. Mater.* **2014**, *26*, 2829.

[3] a) T. W. Kelley, P. F. Baude, C. Gerlach, D. E. Ender, D. Muyres, M. A. Haase, D. E. Vogel, S. D. Theiss, *Chem. Mater.* **2004**, *16*, 4413; b) A. Facchetti, *Nat. Mater.* **2013**, *12*, 598.

[4] a) D. Beljonne, G. Pourtois, C. Silva, E. Hennebicq, L. M. Herz, R. H. Friend, G. D. Scholes, S. Setayesh, K. Müllen, J. L. Brédas, *Proc. Natl. Acad. Sci. USA* **2002**, *99*, 10982; b) J.-L. Brédas, D. Beljonne, V. Coropceanu, J. Cornil, *Chem. Rev.* **2004**, *104*, 4971.

[5] a) Z. G. Zhang, J. Wang, *J. Mater. Chem.* **2012**, *22*, 4178; b) R. Noriega, J. Rivnay, K. Vandewal, F. P. V. Koch, N. Stingelin, P. Smith, M. F. Toney, A. Salleo, *Nat. Mater.* **2013**, *12*, 1038; c) J. Mei, Z. Bao, *Chem. Mater.* **2014**, *26*, 604; d) I. Osaka, M. Saito, T. Koganezawa, K. Takimiya, *Adv. Mater.* **2014**, *26*, 331; e) C.-H. Lee, Y.-Y. Lai, J.-Y. Hsu, P.-K. Huang, Y.-J. Cheng, *Chem. Sci.* **2017**, *8*, 2942.

[6] a) L. Fang, Y. Zhou, Y.-X. Yao, Y. Diao, W.-Y. Lee, A. L. Appleton, R. Allen, J. Reinspach, S. C. B. Mannsfeld, Z. Bao, *Chem. Mater.* **2013**, *25*, 4874; b) T. Lei, J.-Y. Wang, J. Pei, *Chem. Mater.* **2014**, *26*, 594; c) I. Osaka, K. Takimiya, *Polymer* **2015**, *59*, A1.

[7] a) T. Lei, J.-H. Dou, J. Pei, *Adv. Mater.* **2012**, *24*, 6457; b) Z. Yi, S. Wang, Y. Liu, *Adv. Mater.* **2015**, *27*, 3589.

[8] a) I. Meager, R. S. Ashraf, S. Mollinger, B. C. Schroeder, H. Bronstein, D. Beatrup, M. S. Vezie, T. Kirchartz, A. Salleo, J. Nelson, I. McCulloch, *J. Am. Chem. Soc.* **2013**, *135*, 11537; b) J. Y. Back, H. Yu, I. Song, I. Kang, H. Ahn, T. J. Shin, S.-K. Kwon, J. H. Oh, Y.-H. Kim, *Chem. Mater.* **2015**, *27*, 1732.

[9] X. Liu, B. He, C. L. Anderson, J. Kang, T. Chen, J. Chen, S. Feng, L. Zhang, M. A. Kolaczkowski, S. J. Teat, M. A. Brady, C. Zhu, L.-W. Wang, J. Chen, Y. Liu, *J. Am. Chem. Soc.* **2017**, *139*, 8355.

[10] a) G. K. Dutta, A. R. Han, J. Lee, Y. Kim, J. H. Oh, C. Yang, *Adv. Funct. Mater.* **2013**, *23*, 5317; b) G. Kim, S.-J. Kang, G. K. Dutta, Y.-K. Han, T. J. Shin, Y.-Y. Noh, C. Yang, *J. Am. Chem. Soc.* **2014**, *136*, 9477; c) T. Kumari, S. M. Lee, C. Yang, *Adv. Funct. Mater.* **2018**, 1707278.

[11] J.-L. Bredas, *Mater. Horiz.* **2014**, *1*, 17.

[12] X. Zhang, L. J. Richter, D. M. DeLongchamp, R. J. Kline, M. R. Hammond, I. McCulloch, M. Heeney, R. S. Ashraf, J. N. Smith, T. D. Anthopoulos, B. Schroeder, Y. H. Geerts, D. A. Fischer, M. F. Toney, *J. Am. Chem. Soc.* **2011**, *133*, 15073.

[13] a) S. Park, M. H. Lee, K. S. Ahn, H. H. Choi, J. Shin, J. Xu, J. Mei, K. Cho, Z. Bao, D. R. Lee, M. S. Kang, D. H. Kim, *Adv. Funct. Mater.* **2016**, *26*, 4627; b) B. C. Schroeder, T. Kurosawa, T. Fu, Y.-C. Chiu, J. Mun, G.-J. N. Wang, X. Gu, L. Shaw, J. W. E. Kneller, T. Kreouzis, M. F. Toney, Z. Bao, *Adv. Funct. Mater.* **2017**, *27*, 1701973.

[14] Y. Liu, J. Zhao, Z. Li, C. Mu, W. Ma, H. Hu, K. Jiang, H. Lin, H. Ade, H. Yan, *Nat. Commun.* **2014**, *5*, 5293.

[15] G. Xue, X. Zhao, G. Qu, T. Xu, A. Gumyusenge, Z. Zhang, Y. Zhao, Y. Diao, H. Li, J. Mei, *ACS Appl. Mater. Interfaces* **2017**, *9*, 25426.

# ADVANCED FUNCTIONAL MATERIALS

## Reprint Order Form 2018

**Short DOI:  adfm. _____**

Please send me and bill me for

[ ]        **Reprints** via   [ ] airmail (+ 25 Euro)
                              [ ] surface mail

Please send me and bill me for a:

[ ]        **Issue copies** (25 Euro)

[ ]        **high-resolution PDF file** (330 Euro).

My Email address:
_____

Please note: It is not permitted to present the PDF file on the internet or on company homepages.

**Information regarding VAT**
Please note that from German sales tax point of view, the charge for **Reprints, Issues or Posters** is considered as **"supply of goods"** and therefore, in general, such delivery is a subject to German sales tax. However, this regulation has no impact on customers located outside of the European Union. Deliveries to customers outside the Community are automatically tax-exempt. Deliveries within the Community to institutional customers outside of Germany are exempted from the German tax (VAT) only if the customer provides the supplier with his/her VAT number. The VAT number (value added tax identification number) is a tax registration number used in the countries of the European Union to identify corporate entities doing business there. It starts with a country code (e.g. FR for France, GB for Great Britain) and follows by numbers.

**VAT no.:** _____
(Institutes / companies in EU countries only)

**Purchase Order No.:** _____

**Delivery address / Invoice address:**
Name of recipient, University, Institute, Street name and Street number, Postal Code, Country

_____

_____

_____

_____

_____

_____

_____

**Date and Signature:** _____

**Credit Card Payment** (optional)   -You will receive an invoice.

**VISA, MasterCard, AMERICAN EXPRESS**

Please use the Credit Card Token Generator located at the website below to create a token for secure payment. The token will be used instead of your credit card number.

**Credit Card Token Generator:**
https://www.wiley-vch.de/editorial_production/index.php

Please transfer your token number to the space below.

**Credit Card Token Number**

| | | | | | | | | | | | | | | | | |
|---|---|---|---|---|---|---|---|---|---|---|---|---|---|---|---|---|

---

**Price list for reprints** (The prices include mailing and handling charges. All Wiley-VCH prices are exclusive of VAT)

| No. of pages | Price (in Euro) for orders of | | | | | |
| --- | --- | --- | --- | --- | --- | --- |
| | 50 copies | 100 copies | 150 copies | 200 copies | 300 copies | 500 copies |
| 1-4 | 345 | 395 | 425 | 445 | 548 | 752 |
| 5-8 | 490 | 573 | 608 | 636 | 784 | 1077 |
| 9-12 | 640 | 739 | 786 | 824 | 1016 | 1396 |
| 13-16 | 780 | 900 | 958 | 1004 | 1237 | 1701 |
| 17-20 | 930 | 1070 | 1138 | 1196 | 1489 | 2022 |
| for every additional 4 pages | 147 | 169 | 175 | 188 | 231 | 315 |

**WILEY-VCH**